



HAL
open science

A 15-GHz reconfigurable calibration-free linear FMCW chirp generator with type-III nested-PLL

Xuan Wang, Yupeng Fu, Xujun Ma, Dongming Wang, Xu Wu, Lianming Li

► **To cite this version:**

Xuan Wang, Yupeng Fu, Xujun Ma, Dongming Wang, Xu Wu, et al.. A 15-GHz reconfigurable calibration-free linear FMCW chirp generator with type-III nested-PLL. 2023 Asia-Pacific Microwave Conference (APMC), Dec 2023, Taipei, China. pp.602-604, 10.1109/APMC57107.2023.10439799 . hal-04872805

HAL Id: hal-04872805

<https://hal.science/hal-04872805v1>

Submitted on 8 Jan 2025

HAL is a multi-disciplinary open access archive for the deposit and dissemination of scientific research documents, whether they are published or not. The documents may come from teaching and research institutions in France or abroad, or from public or private research centers.

L'archive ouverte pluridisciplinaire **HAL**, est destinée au dépôt et à la diffusion de documents scientifiques de niveau recherche, publiés ou non, émanant des établissements d'enseignement et de recherche français ou étrangers, des laboratoires publics ou privés.

A 15-GHz Reconfigurable Calibration-Free Linear FMCW Chirp Generator with Type-III Nested-PLL

Xuan Wang
Southeast University
Purple Mountains Laboratories
Nanjing, China
230198089@seu.edu.cn

Yupeng Fu
Naval Aeronautical University
Yantai, China
230169616@seu.edu.cn

Xujun Ma
Télécom SudParis
Institut Polytechnique de Paris
Palaiseau, France
xujun.ma@telecom-sudparis.eu

Dongming Wang
Southeast University
Purple Mountains Laboratories
Nanjing, China
wangdm@seu.edu.cn

Xu Wu
Southeast University
Purple Mountains Laboratories
Nanjing, China
xu.wu@seu.edu.cn

Lianming Li
Southeast University
Purple Mountains Laboratories
Nanjing, China
Lianming.Li@seu.edu.cn

Abstract—A 15-GHz reconfigurable calibration-free frequency synthesizer is proposed for linear frequency-modulated continuous-wave (FMCW) chirp generation. By utilizing the type-III PLL architecture to adaptively track the ramp, the chirp linearity is improved remarkably for wide bandwidth operation. In addition, to further reduce the quantization noise from delta-sigma modulation (DSM) and suppress the in-band noise folding effect, a nested-PLL architecture is leveraged. Implemented in a 65-nm CMOS process, the proposed FMCW chirp generator consumes 55 mW power and supports triangular and sawtooth waveforms. Measurement results show that the phase noise of 15.17 GHz carrier frequency is -97.8 dBc/Hz at 1 MHz offset. Without any efforts in calibration, the chirp generator achieves 1 GHz chirp bandwidth and 25 μ s chirp period with a root-mean-square (RMS) frequency error as low as 341 kHz.

Keywords—linear frequency-modulated continuous-wave (FMCW) chirp generation, nested-PLL, type-III architecture

I. INTRODUCTION

Millimeter-wave (mm-Wave) FMCW radar has achieved a great success in various sensing scenarios such as 3-D imaging, autonomous-driving and biological detection [1]. As the key building block of the FMCW radar system, FMCW chirp generator plays a critical role in enabling reliable radar sensing, but its performance always presents a bottleneck in such applications.

To reduce the phase noise and extend the sweep bandwidth while improving the chirp linearity, several FMCW chirp generators have been proposed in recent years. Conventional fractional-N charge-pump phase-locked loop (CP-PLL) is widely used in the radar system [2]-[4], but it suffers from a limited chirp slope, since this architecture contains a narrow-bandwidth loop to suppress the quantization noise from the delta-sigma modulation (DSM) and in-band noise folding effect [5]. Typically, to increase chirp bandwidth, charge-pump (CP) should have a large dynamic voltage range, but it is hard to achieve high linearity and low phase noise simultaneously over the entire CP voltage range. Alternatively, digital-to-time converter (DTC) based sub-sampling PLLs (SSPLL) and two-point-modulation (TPM) technique are introduced for better linearity and phase noise performance [6]-[7]. However, the gain error of DTC and the time and gain mismatches between two modulated paths need to be calibrated by complex methods through strict procedures. Besides, the frequency acquisition range is limited and an extra FLL is necessary. With features of flexible configuration, high compatibility and scalable size, several all-digital PLL (ADPLL) based FMCWs are presented [8]-[9]. Though a high

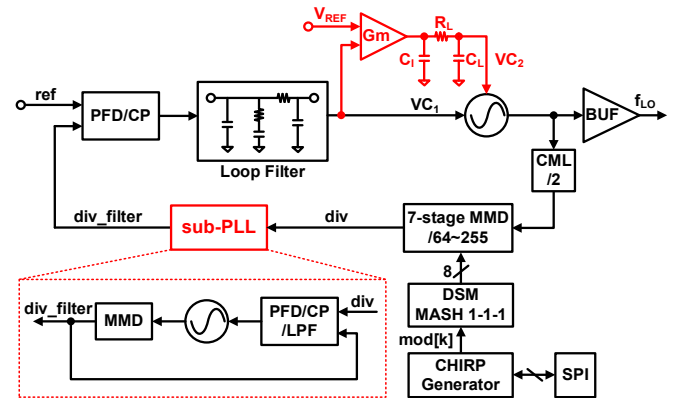


Fig. 1. Architecture of the proposed FMCW chirp generator.

chirp linearity is achieved, the performance of time-to-digital converter (TDC) and phase-interpolator (PI) are quite sensitive to the circuit parasitics, posing difficulties in the chip implementation.

This paper presents a 15-GHz reconfigurable calibration-free frequency synthesizer with wide bandwidth and high linearity. To avoid complex calibration and improve lock acquisition ability, a CP-PLL is utilized as the main structure. In the proposed PLL, a self-adaptive loop is utilized to improve the chirp linearity and a nested-PLL architecture is adopted to suppress the DSM quantization noise and in-band noise folding effect. For different applications, triangular and sawtooth chirps can be configured through the serial peripheral interface (SPI). Moreover, advantages of the proposed type-III nested-PLL are proved through simulation and measurement against the conventional CP-PLL.

II. PROPOSED 15-GHz CALIBRATION-FREE LINEAR FMCW CHIRP GENERATOR

A. System Architecture

Fig. 1 shows the block diagram of the proposed 15-GHz calibration-free linear FMCW chirp generator, which could be further multiplied by a quadrupler to drive a 60-GHz radar transceiver. The choice of such a low carrier frequency relaxes the VCO and frequency divider chain design. The 15 GHz VCO output is first processed by a divide-by-2 current-mode logic (CML) frequency divider and then sent to the multi-modulus frequency divider (MMD) to generate the division signal. The chirp generator is controlled by SPI to generate the $\text{mod}[k]$ signal for the MASH 1-1-1 DSM, which modulates the MMD to obtain a targeted fractional division ratio. To further suppress the DSM quantization noise, a sub-PLL is

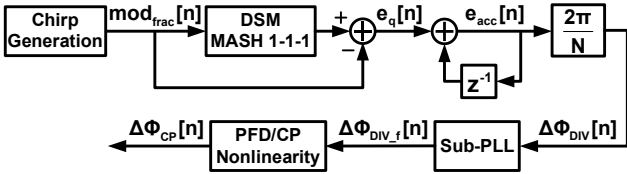


Fig. 2. Block diagram of the Simulink simulation model with PFD/CP nonlinearity in the loop.

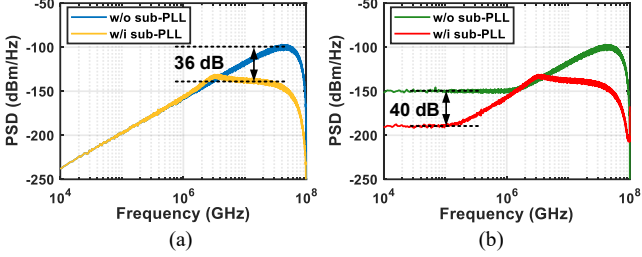


Fig. 3. Simulated PSD of the equivalent phase error at the PFD/CP output (a) when PFD/CP is linear and (b) when PFD/CP is nonlinear.

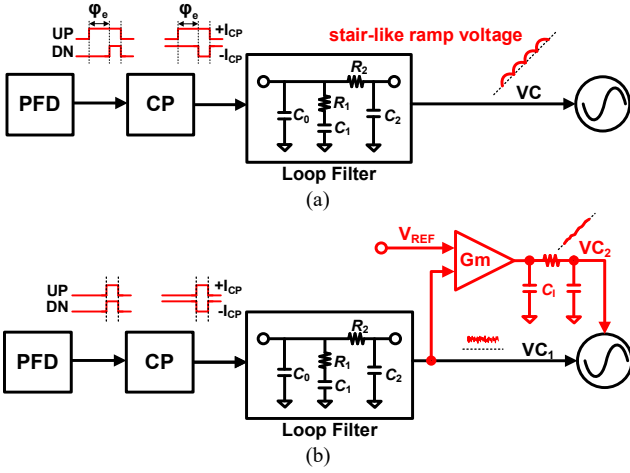


Fig. 4. Ramp generation mechanisms based on different architectures. (a) Conventional type-II architecture. (b) Proposed type-III architecture with an adaptive ramp tracking loop.

integrated to filter the division signal. For the chirp generation, in this design a type-III architecture is adopted by paralleling an additional feedback loop, thereby adaptively tracking the ramp without calibration. With the transconductance amplifier G_m and integral capacitor C_1 , an G_m - C_1 integrator circuit is realized, and the linearity of the control voltage VC_2 is improved remarkably. Furthermore, an R_L - C_L low-pass filter is utilized in this G_m - C_1 integrator for anti-aliasing purposes.

B. Quantization Noise and In-Band Noise Folding Effect Suppression with Sub-PLL

In order to evaluate the suppression of quantization noise and in-band noise folding effect, a Simulink simulation model is established by considering the nonlinearity effects in Fig. 2, where the quantization error $e_q[n]$ is introduced to quantify the frequency error in the loop. With the accumulation of $e_q[n]$, the accumulated error $e_{acc}[n]$ directly contributes to the PLL phase noise. As shown in Fig. 3(a), without considering the nonlinearity of PFD/CP, the power spectral density (PSD) of the equivalent phase error at the PFD/CP output is decreased by about 36 dB at $f_{ref}/2$ offset. Furthermore, by introducing 1% mismatch between CP I_{UP} and I_{DN} current, the in-band phase noise could be further improved by 40 dB benefiting from the use of sub-PLL, as indicated in Fig. 3(b).

C. Linearity Improvement with Adaptive Ramp Tracking of Type-III Architecture

In this design, the type-III architecture outperforms the conventional type-II architecture in aspects of adaptive ramp-tracking capability and chirp linearity. Fig. 4 demonstrates ramp generation mechanisms using Type-II and Type-III architectures for performance comparison, without considering the DSM quantization noise. As shown in Fig. 4(a), the conventional type-II architecture inevitably suffers from a fixed phase error φ_e when it generates the up/down sweep voltage for VCO in the chirp mode. According to [10], the phase error φ_e increases with the chirp slope. Furthermore, after the periodic pulsed current is injected into the low-pass loop filter (LPF), a stair-like sweep voltage will be generated for VCO tuning, causing periodic frequency error.

In contrast, the proposed type-III architecture is shown in Fig. 4(b). By shunting the G_m - C_1 integrator across the separated VCO control voltages, i.e., VC_1 and VC_2 , an additional negative feedback loop is realized. To illustrate the working mechanism, the up ramp generation is explained below. If the output current I_{Gm} of G_m is higher than the expected value, a faster chirp slope is induced and a negative phase error φ_e will be detected by the PFD, thus generating a correction signal to compensate VC_1 and reducing I_{Gm} through the negative feedback loop. Eventually, the phase error φ_e will converge to zero, and VC_1 maintains a constant value, while VC_2 is integrated smoothly into a steady chirp state.

III. MEASUREMENT RESULTS

As shown in Fig. 5, the proposed FMCW chirp generator is fabricated in a 65-nm CMOS process and the chip area is about 2.47 mm^2 . With 0.8 V supply voltage for VCO, 1.8 V for G_m and CP and 1.2 V for the rest circuits, the total power consumption is 55 mW.

Fig. 6 shows the measured phase noise performance in the single tone test. As indicated, the phase noise of 15.17 GHz carrier frequency is -97.8 dBc/Hz at 1 MHz offset. The chirp

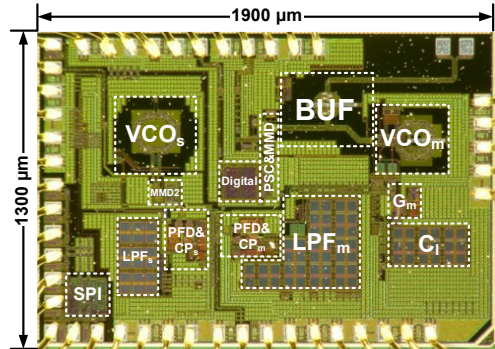


Fig. 5. Chip microphotograph of the proposed FMCW chirp generator.

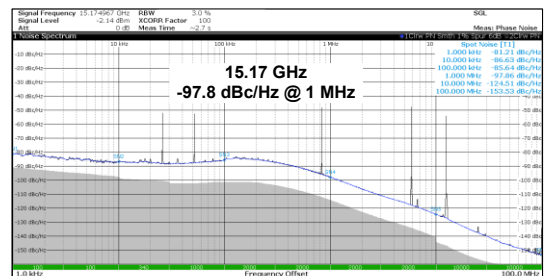


Fig. 6. Measured PLL phase noise.

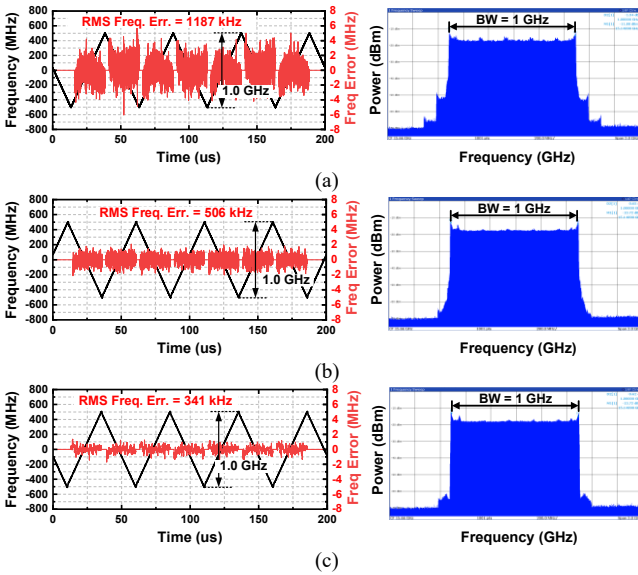


Fig. 7. Measured frequency error and spectrum of FMCW chirps with 1 GHz bandwidth and 25 μ s chirp period in different PLL architectures: (a) conventional type-II architecture; (b) type-III architecture without sub-PLL; (c) type-III architecture with sub-PLL.

signal is measured by the R&S FSW67 signal and spectrum analyzer. By configuring the PLL with different architectures to generate the same triangular chirp with 1 GHz bandwidth and 25 μ s chirp period, the measured chirp waveform, frequency error, and spectrum are compared in Fig. 7. As shown in Fig. 7(a), for the conventional type-II PLL without sub-PLL, its RMS frequency error is 1187 kHz. With the type-III architecture, the RMS frequency error could be reduced to 506 kHz in Fig. 7(b). Furthermore, as indicated in Fig. 7(c), for the proposed type-III architecture with sub-PLL, its RMS frequency error is reduced to 341 kHz. Moreover, benefiting from the type-III architecture, the reference spur over the chirp frequency range is attenuated greatly, while the fractional spur at the chirp edge is also suppressed.

TABLE I. PERFORMANCE COMPARISON WITH THE STATE-OF-THE-ART RESULTS

| | This work | | [9] | [2] | [11] |
|-------------------------------------|-----------------------|-------|----------------|---------------|----------------------|
| Architecture | Type III /Nested Loop | | ADPLL /TPM | Analog | Type III /Mixed-Mode |
| Process | 65 nm CMOS | | 40 nm CMOS | 65 nm CMOS | 65 nm CMOS |
| Calibration | NO | | NO | NO | NO |
| Freq. range [GHz] | 14.0-16.6 | | 11.7-13.5 | 76.0-76.7 | 77-78.83 |
| Reference [MHz] | 100 | | 100 | 267.6 | 125 |
| Phase Noise [dBc/Hz] | -97.8 /-85.8* | | -113.6 /-99.6* | -85.1 /-87.3* | -81.7 /-83.9* |
| BW_{chirp} [GHz] | 1.0 /4.0* | | 0.3 /1.5* | 0.69 /0.53* | 1.83 /1.43* |
| T_{chirp} [μs] | 100 | 25 | 3.85 | 1413 | 1000 |
| RMS F_{error} [kHz] | 128 | 341 | 167 | <73 | 336 |
| Chirp slope [MHz/μs] | 40* | 160* | 390* | 0.38* | 1.42* |
| RMS F_{error}/BW [%] | 0.012 | 0.034 | 0.056 | <0.01 | 0.018 |
| Power [mW] | 55 | | 33.8 | 51.3 | 43.1 |

*Normalized to 60 GHz frequency band.

Table I summarizes the performance of the proposed FMCW chirp generator and the state-of-the-art works without calibration. As indicated, the proposed FMCW chirp generator could provide a maximum sweep bandwidth of 1 GHz, which can be further extended to 4 GHz by a quadrupler for the targeting 60 GHz band operation with a very low frequency error.

IV. CONCLUSION

In this paper, a 15-GHz reconfigurable calibration-free linear FMCW chirp generator with type-III nested-PLL is proposed. A type-III architecture is utilized for adaptive ramp tracking, which improves the chirp linearity greatly. A sub-PLL is employed to suppress the DSM quantization noise and the in-band noise folding effect. Fabricated in a 65-nm CMOS process, measurement results show that the proposed FMCW chirp generator supports triangular and sawtooth waveforms, and achieves 1 GHz bandwidth over 25 μ s period with a root-mean-square (RMS) frequency error as low as 341 kHz.

ACKNOWLEDGMENT

This work was supported by the National Key R&D Program of China with Grant No. 2018YFE0205900 and the Major Key Project of PCL(PCL2021A01-2).

REFERENCES

- [1] L. Lu, X. Ma, Y. Liang, Z. Liu, X. Fan and L. Li, "A 60-GHz Hybrid FMCW-Doppler Radar for Vibration Detection With a Robust I/Q Calibration Method," in *IEEE Sensors Journal*, vol. 22, no. 21, pp. 20464-20474, Nov. 2022.
- [2] T. -N. Luo, C. -H. E. Wu and Y. -J. E. Chen, "A 77-GHz CMOS FMCW Frequency Synthesizer With Reconfigurable Chirps," *IEEE Trans. Microw. Theory Techn.*, vol. 61, no. 7, pp. 2641-2647, July 2013.
- [3] H. Jia et al., "A 77 GHz frequency doubling two-path phased-array FMCW transceiver for automotive radar," *IEEE J. Solid-State Circuits*, vol. 51, no. 10, pp. 2299-2311, Oct. 2016.
- [4] J. Park, H. Ryu, K. -W. Ha, J. -G. Kim and D. Baek, "76-81-GHz CMOS Transmitter With a Phase-Locked-Loop-Based Multi chirp Modulator for Automotive Radar," *IEEE Trans. Microw. Theory Techn.*, vol. 63, no. 4, pp. 1399-1408, April 2015.
- [5] V. Mazzaro and M. P. Kennedy, "Folded Noise Prediction in Nonlinear Fractional-N Frequency Synthesizers," *IEEE Trans. Circuits Syst. I, Reg. Papers*, vol. 68, no. 10, pp. 4038-4048, Oct. 2021.
- [6] Q. Shi, K. Bunsen, N. Markulic and J. Craninckx, "A self-calibrated 16-GHz subsampling-PLL-based fast-chirp FMCW modulator with 1.5-GHz bandwidth," *IEEE J. Solid-State Circuits*, vol. 54, no. 12, pp. 3503-3512, Dec. 2019.
- [7] P. T. Renukaswamy, N. Markulic, P. Wambacq, and J. Craninckx, "A 12-mW 10-GHz FMCW PLL based on an integrating DAC with 28-kHz RMS-frequency-error for 23-MHz/ μ s slope and 1.2-GHz chirp bandwidth," *IEEE J. Solid-State Circuits*, vol. 55, no. 12, pp. 3294-3307, Dec. 2020.
- [8] J. Wu et al., "A 77-GHz Mixed-Mode FMCW Generator Based on a Vernier TDC With Dual Rising-Edge Fractional-Phase Detector," *IEEE Trans. Circuits Syst. I, Reg. Papers*, vol. 67, no. 1, pp. 60-73, Jan. 2020.
- [9] Z. Shen et al., "A 12-GHz Calibration-Free All-Digital PLL for FMCW Signal Generation With 78 MHz/ μ s Chirp Slope and High Chirp Linearity," *IEEE Trans. Circuits Syst. I, Reg. Papers*, vol. 67, no. 12, pp. 4445-4456, Dec. 2020.
- [10] A. Ergintav, F. Herzel, D. Kissinger and H. J. Ng, "An Investigation of the Phase Noise of a Fractional-N PLL in the Course of FMCW Chirp Generation," *Proc. IEEE Int. Symp. Circuits Syst. (ISCAS)*, pp. 1-4, 2018.
- [11] J. Lin, Z. Song, N. Qi, W. Rhee, Z. Wang and B. Chi, "A 77-GHz Mixed-Mode FMCW Signal Generator Based on Bang-Bang Phase Detector," *IEEE J. Solid-State Circuits*, vol. 53, no. 10, pp. 2850-2863, Oct. 2018.